

A SIMPLE ANALYTICAL METHOD TO DETERMINE SOLAR ENERGETIC PARTICLES' MEAN FREE PATH

H.-Q. HE¹ AND G. QIN

State Key Laboratory of Space Weather, Center for Space Science and Applied Research, Chinese Academy of Sciences, Beijing 100190, China;
hqhe@spaceweather.ac.cn, gqin@spaceweather.ac.cn

Received 2010 November 29; accepted 2011 January 18; published 2011 March 3

ABSTRACT

To obtain the mean free path of solar energetic particles (SEPs) for a solar event, one usually has to fit time profiles of both flux and anisotropy from spacecraft observations to numerical simulations of SEPs' transport processes. This method can be called a simulation method. But a reasonably good fitting needs a lot of simulations, which demand a large amount of calculation resources. Sometimes, it is necessary to find an easy way to obtain the mean free path of SEPs quickly, for example, in space weather practice. Recently, Shalchi et al. provided an approximate analytical formula of SEPs' anisotropy time profile as a function of particles' mean free path for impulsive events. In this paper, we determine SEPs' mean free path by fitting the anisotropy time profiles from Shalchi et al.'s analytical formula to spacecraft observations. This new method can be called an analytical method. In addition, we obtain SEPs' mean free path with the traditional simulation methods. Finally, we compare the mean free path obtained with the simulation method to that of the analytical method to show that the analytical method, with some minor modifications, can give us a good, quick approximation of SEPs' mean free path for impulsive events.

Key words: interplanetary medium – magnetic fields – Sun: coronal mass ejections (CMEs) – Sun: flares – Sun: particle emission

1. INTRODUCTION

Cosmic rays' transport in interplanetary space is one of the fundamental problems of astrophysics. It is the basic knowledge needed to study space weather. Parker (1965) provided a transport equation for charged particles with diffusion to study cosmic-ray modulation. Furthermore, to study solar energetic particles (SEPs), a focused transport equation was obtained (Parker 1963; Roelof 1969; Ng & Reames 1994). It is very difficult to solve the particle transport equation analytically; therefore, numerical solutions are usually used (e.g., Ng & Wong 1979; Schlüter 1985; Ruffolo 1991; Kocharov et al. 1998; Qin et al. 2005, 2006; Zhang et al. 2009; Dröge & Kartavykh 2009; He et al. 2011). To study charged particles' transport, we have to understand their diffusion mechanism. Jokipii (1966) developed a quasi-linear theory (QLT) for cosmic ray diffusion, from which it is obtained that the perpendicular diffusion coefficient is much smaller than the parallel one in weak magnetic turbulence. Therefore, in the study of the transport of SEPs in interplanetary space, perpendicular diffusion is usually ignored in favor of parallel diffusion. However, Dwyer et al. (1997) and Zhang et al. (2003) reported that perpendicular diffusion could be comparable to parallel diffusion. In addition, simulations show that with turbulence levels $\lesssim 1$, perpendicular diffusion is much smaller than parallel diffusion (e.g., Qin 2002; Qin et al. 2002), but with turbulence levels $\gg 1$, perpendicular diffusion could exceed parallel diffusion (G. Qin 2005, private communication; results published in Shalchi 2005b). Furthermore, there are theories considering nonlinear effects that agree well with numerical simulations (Matthaeus et al. 2003; Shalchi et al. 2004; Qin 2007), and Shalchi (2008) provided a simple explanation of large perpendicular diffusion coefficients.

SEPs' mean free path, determined by physical properties of SEPs as well as those of solar wind, is a very important parameter in space physics to study the transport of energetic particles in

the heliosphere, especially for space weather prediction (e.g., Qin et al. 2009). In order to accurately obtain the mean free path of SEPs for a solar event, a method of fitting time profiles of both flux and anisotropy from spacecraft observations to numerical simulations of SEPs' transport processes has to be used. This can be called a simulation method. However, a reasonably good fitting usually needs many simulations, which demand a large amount of calculation resources and are time-consuming even with modern supercomputers. It is necessary to find an alternative way to approximately estimate the mean free path of SEPs quickly, especially in space weather forecasting. Recently, Shalchi et al. (2009) developed an approximate analytical formula of SEPs' anisotropy time profile as a function of particles' mean free path for impulsive events. It is possible to obtain SEPs' mean free path by fitting the analytical formula to SEPs' anisotropy time profile observed by spacecraft without adopting the time-consuming simulations of particles' transport processes.

In this paper, we use an analytical method to determine SEPs' mean free path by fitting the anisotropy profile from the approximate analytical formula of Shalchi et al. (2009) to spacecraft observations for three impulsive SEP events with different conditions. In addition, for each event, we obtain SEPs' mean free path with traditional simulation methods. Afterward, we compare the mean free path obtained with the traditional simulation methods to that obtained with the new analytical method to check the validity of the analytical method.

2. MODEL

In order to obtain an analytical form of anisotropy profiles of SEPs, Shalchi et al. (2009) used a simple two-dimensional Fokker–Planck equation that governs the gyrophase-averaged distribution function $f(z, \mu, t)$ of SEPs (e.g., Skilling 1971; Schlickeiser 2002; Qin et al. 2005):

$$\frac{\partial f}{\partial t} + \mu v \frac{\partial f}{\partial z} = \frac{\partial}{\partial \mu} \left(D_{\mu\mu} \frac{\partial f}{\partial \mu} \right), \quad (1)$$

¹ Also at: Graduate University of Chinese Academy of Sciences, Beijing 100049, China.

where z is the coordinate along the magnetic field spiral, μ is a particle's pitch-angle cosine, t is time, and v is the particle speed.

It is assumed that the parallel mean free path λ_{\parallel} can be written as (Jokipii 1966; Hasselmann & Wibberenz 1968, 1970; Earl 1974)

$$\lambda_{\parallel} = \frac{3v}{8} \int_{-1}^{+1} \frac{(1 - \mu^2)^2}{D_{\mu\mu}} d\mu, \quad (2)$$

and the radial mean free path can be defined as (e.g., Bieber et al. 1994)

$$\lambda_r = \lambda_{\parallel} \cos^2 \psi, \quad (3)$$

where ψ is the angle between the local magnetic field direction and the radial direction.

For simplicity, a general form of the pitch-angle diffusion coefficient can be used (Beeck & Wibberenz 1986; Qin et al. 2005):

$$D_{\mu\mu} = D(1 - \mu^2)\{|\mu|^{q-1} + h\}, \quad (4)$$

where D is a constant indicating the magnetic field fluctuation level. The constant q is related to the power spectrum of magnetic field turbulence in the inertial range. The constant h is needed to simulate the particles' ability to scatter through $\mu = 0$ because of nonlinear effects. As we know, in solar wind without too-weak magnetic turbulence, charged particles encounter considerable scattering at $\mu = 0$, so that in the pitch-angle diffusion models $h \gg 0$ (e.g., Qin & Shalchi 2009). Alternatively, we can use a more general form of the pitch-angle diffusion coefficient, derived analytically by Shalchi et al. (2009) as

$$D_{\mu\mu} = \frac{\pi D(s, q)}{2s} (1 - \mu^2) \frac{v}{l_{\text{slab}}} R^{s-2} \frac{\delta B}{B_0} \times \sum_{n=\pm 1} \text{sign} \left(\frac{\delta B}{B_0} + n|\mu| \right) \cdot \left| |\mu| + n \frac{\delta B}{B_0} \right|^s, \quad (5)$$

which could be applied to pitch-angle scattering for both weak and strong turbulence. The discussion of this formula may be our future work.

Based on the second-order QLT of Shalchi (2005a), Shalchi et al. (2009) used an isotropic form of the pitch-angle diffusion coefficient with strong nonlinear effects:

$$D_{\mu\mu} = D(1 - \mu^2), \quad (6)$$

i.e., when $h \gg 1$ in Equation (4). The standard QLT provides $D_{\mu\mu}(\mu = 0) = 0$. This problem is known as the 90° problem of scattering theory. One can avoid such a problem by using the isotropic form in Equation (6); for more details, please refer to Shalchi (2009).

For impulsive events, by computing the spatial average,

$$F(\mu, t) = \int_{-\infty}^{+\infty} f(\mu, z, t) dz, \quad (7)$$

and adopting Legendre polynomials, Shalchi et al. (2009) obtained an approximate analytical formula of SEPs' anisotropy time profile as a function of particles' mean free path:

$$A(t) = 3\mu_0 e^{-vt/\lambda_{\parallel}}. \quad (8)$$

By fitting the anisotropy time profile from this analytical formula to spacecraft observations, we can roughly determine SEPs' mean free path. This method can be called the analytical method.

Furthermore, we also use traditional simulation methods to accurately obtain the mean free path of SEPs by fitting time profiles of both flux and anisotropy from numerical simulations of SEPs' transport processes to spacecraft observations. In our simulations, we compare results from different models of the pitch-angle diffusion coefficient by varying q and h in Equation (4): (1) $h \gg 1$, i.e., Equation (6); (2) $q = 5/3$ and $h = 0.05$, i.e.,

$$D_{\mu\mu} = D(1 - \mu^2)\{\mu^{2/3} + 0.05\}; \quad (9)$$

and (3) $q = 5/3$ and $h = 0.2$, i.e.,

$$D_{\mu\mu} = D(1 - \mu^2)\{\mu^{2/3} + 0.2\}. \quad (10)$$

Note that the pitch-angle diffusion models used in the simulations, including Equation (6), which is also used to derive the analytical method, have stronger scattering near $\mu \rightarrow 0$ because of nonlinear effects. In our simulations, we also assume particles have a constant radial mean free path, λ_r , propagating through the heliosphere (Bieber et al. 1994).

We apply the time-backward Markov stochastic-process method (Zhang 1999; Qin et al. 2006) to solve the two-dimensional Fokker-Planck formula (Equation (1)):

$$\frac{\partial f}{\partial t} + \mu v \frac{\partial f}{\partial z} + \mathbf{V}^{\text{sw}} \cdot \nabla f = -\frac{d\mu}{dt} \frac{\partial f}{\partial \mu} + \frac{\partial}{\partial \mu} \left(D_{\mu\mu} \frac{\partial f}{\partial \mu} \right) + Q(\mathbf{x}, t), \quad (11)$$

where \mathbf{x} is a particle's position, \mathbf{V}^{sw} is the solar wind velocity, and Q is the source term. In addition, $d\mu/dt$, which includes the magnetic focusing effect and the divergence of the solar wind-flows effect, can be written as (e.g., Roelof 1969; Isenberg 1997; Kóta 1997)

$$\frac{d\mu}{dt} = \frac{1 - \mu^2}{2} \left[-\frac{v}{B} \frac{\partial B}{\partial z} + \mu \left(\frac{\partial V_x^{\text{sw}}}{\partial x} + \frac{\partial V_y^{\text{sw}}}{\partial y} - 2 \frac{\partial V_z^{\text{sw}}}{\partial z} \right) \right] = \frac{1 - \mu^2}{2} \left[\frac{v}{L} + \mu \left(\frac{\partial V_x^{\text{sw}}}{\partial x} + \frac{\partial V_y^{\text{sw}}}{\partial y} - 2 \frac{\partial V_z^{\text{sw}}}{\partial z} \right) \right], \quad (12)$$

where B is the background interplanetary magnetic field in the \mathbf{z} direction and the magnetic focusing length L is defined by $L = (\mathbf{z} \cdot \nabla \ln B)^{-1}$. The source particles with power-law spectrum γ injected at $r < 0.05$ AU are represented by a Reid-Axford profile (Reid 1964):

$$Q(z < 0.05 \text{ AU}, t) = \frac{C}{t} \exp \left(-\frac{\tau_c}{t} - \frac{t}{\tau_L} \right), \quad (13)$$

where τ_c and τ_L indicate the rise and decay timescales, respectively. An outer escape boundary is set at $r = 50$ AU.

The time-backward Markov stochastic-process method deals easily with an expanded source energy spectrum. When using this method, we trace SEPs back to the initial time, and only those particles in the source region at the initial time contribute to the statistics. The solution of the particle transport equation is obtained in terms of a time-backward Ito stochastic-differential equation (see Gardiner 1983; Freidlin 1985; Zhang 1999); for a detailed description of the method, please refer to Qin et al. (2006).

To get simulation results for SEPs' flux and anisotropy profiles for each case, we calculate 1.5×10^7 particles via a supercomputer with Message Passing Interface.

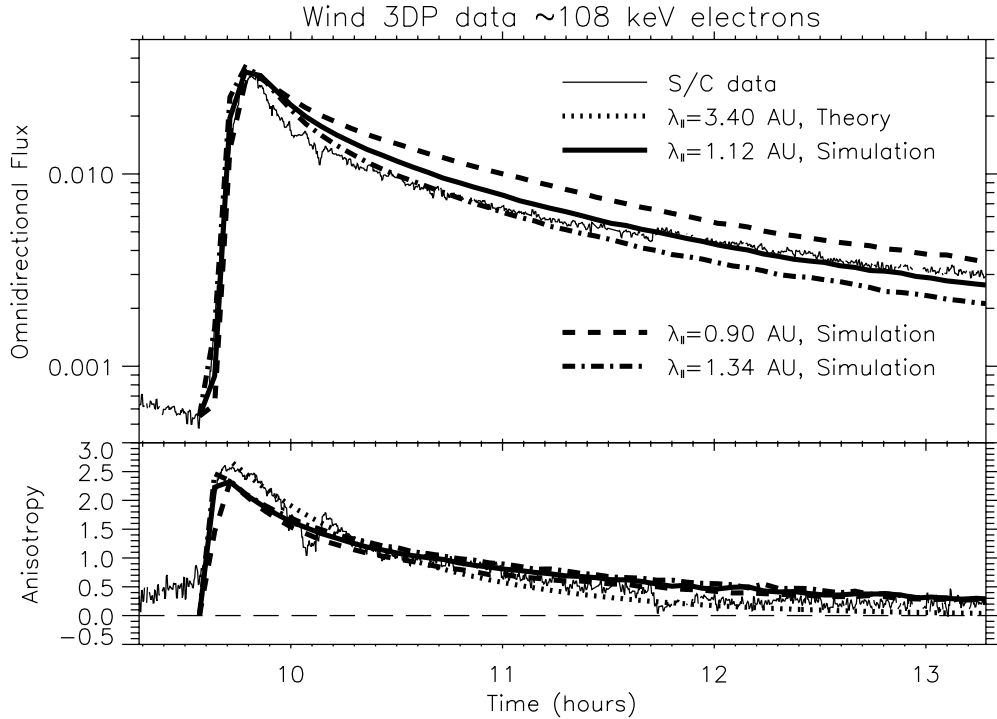


Figure 1. Fits to the flux and anisotropy profiles of *Wind* 3DP ~ 108 keV electron data of the 2000 February 18 event. The form of the pitch-angle diffusion coefficient in Equation (9) is applied in the simulations.

According to the interplanetary background during the three impulsive SEP events observed by the *Wind* spacecraft, the Parker field \mathbf{B} is set so that its magnitude is 5 nT at 1 AU; in addition, solar wind is set to a radial flow, with $V^{\text{sw}} = 380 \text{ km s}^{-1}$. Accordingly, the magnetic footpoint of the nominal field line connecting *Wind* to the Sun is at $\sim \text{W}56^\circ$ (west heliographic longitude 56°), and the angle between the local magnetic field direction and the radial direction, ψ , at 1 AU is $\sim 48^\circ$.

3. RESULTS

In this paper, we study the three impulsive SEP events observed by the three-dimensional Plasma and Energetic Particles (3DP) instrument with an ~ 108 keV electron channel (Lin et al. 1995) on the *Wind* spacecraft. We assume that spacecraft data are observed at 1 AU. We choose SEPs with energy strong enough to avoid local effects, such as interplanetary shock acceleration, adiabatic cooling, etc. To simulate the cases by solving the particle transport formula (Equation (11)), we first apply the form of the pitch-angle diffusion coefficient presented in Equation (9).

The first impulsive SEP event we study is the 2000 February 18 solar event observed by the *Wind* 3DP, Case 1. The solar flare associated with this event occurred on $\sim 09:20$ UT at S16W78. Figure 1 shows fits to the flux and anisotropy profiles of the *Wind* 3DP ~ 108 keV electron data of this event. In these simulations, we choose $\tau_c = 1$ minute and $\tau_L = 80$ minutes in Equation (13). For the two panels, thin solid lines indicate the spacecraft data and thick solid, dashed, and dash-dotted curves indicate three simulations with different mean free paths. The thick solid lines indicate a simulation with a parallel mean free path of $\lambda_{\parallel}^s = 1.12$ AU at 1 AU (corresponding to $\lambda_r = 0.50$ AU), and the dashed and dash-dotted lines indicate simulations with parallel mean free paths of $\lambda_{\parallel}^s = 0.90$ AU at 1 AU (corresponding to $\lambda_r = 0.40$ AU) and $\lambda_{\parallel}^s = 1.34$ AU at 1 AU

(corresponding to $\lambda_r = 0.60$ AU), respectively. We can see that, among the three simulations, the thick solid curves fit the observations best, the dashed and dash-dotted lines corresponding to the upper and lower limits of the parallel mean free path from the simulation method, i.e., $\lambda_{\parallel}^s = 1.12 \pm 0.22$ AU at 1 AU. The dotted line in the bottom panel of the figure indicates the theoretical result of anisotropy obtained from solving the two-dimensional Fokker-Planck formula (Equation (1)) analytically (Shalchi et al. 2009). By fitting the analytical results to observations, we obtain $\mu_0 = 0.89$ and $\lambda_{\parallel}^a = 3.40$ AU in Equation (8). Usually, we get a more definite value of the parallel mean free path with the analytical method, so we do not show the range of results of λ_{\parallel}^a . From the above results, we can get the ratio of the parallel mean free paths of the simulation to theoretical methods, $k_1 = \lambda_{\parallel}^s / \lambda_{\parallel}^a \sim (1.12 \pm 0.22) / 3.40 = 0.32 \pm 0.06$, at 1 AU.

The second impulsive SEP event we study is the 2000 April 4 solar event observed by the *Wind* 3DP, Case 2. The solar flare associated with this event occurred on $\sim 15:00$ UT at N16W66. We also choose the ~ 108 keV electron channel. Figure 2 shows fits to the flux and anisotropy profiles of this event. In these simulations, we choose $\tau_c = 5$ minutes and $\tau_L = 50$ minutes in Equation (13). As shown in the figure, the thick solid curves ($\lambda_{\parallel}^s = 0.56$ AU at 1 AU, i.e., $\lambda_r = 0.25$ AU) fit the observation data best. The thick dashed and dash-dotted lines indicate the simulations that are fit to observations to get the lower and upper limits of the parallel mean free paths, i.e., $\lambda_{\parallel}^s = 0.45$ AU at 1 AU (corresponding to $\lambda_r = 0.20$ AU) and $\lambda_{\parallel}^s = 0.67$ AU at 1 AU (corresponding to $\lambda_r = 0.30$ AU), respectively. The dotted line in the bottom panel indicates the theoretical result of SEPs' anisotropy. By fitting this analytical result to observations, we obtain that $\mu_0 = 0.83$ and $\lambda_{\parallel}^a = 1.70$ AU in Equation (8). For Case 2, the ratio of parallel mean free paths of the simulations to the analytical method is $k_2 = \lambda_{\parallel}^s / \lambda_{\parallel}^a = (0.56 \pm 0.11) / 1.70 = 0.33 \pm 0.06$ AU.

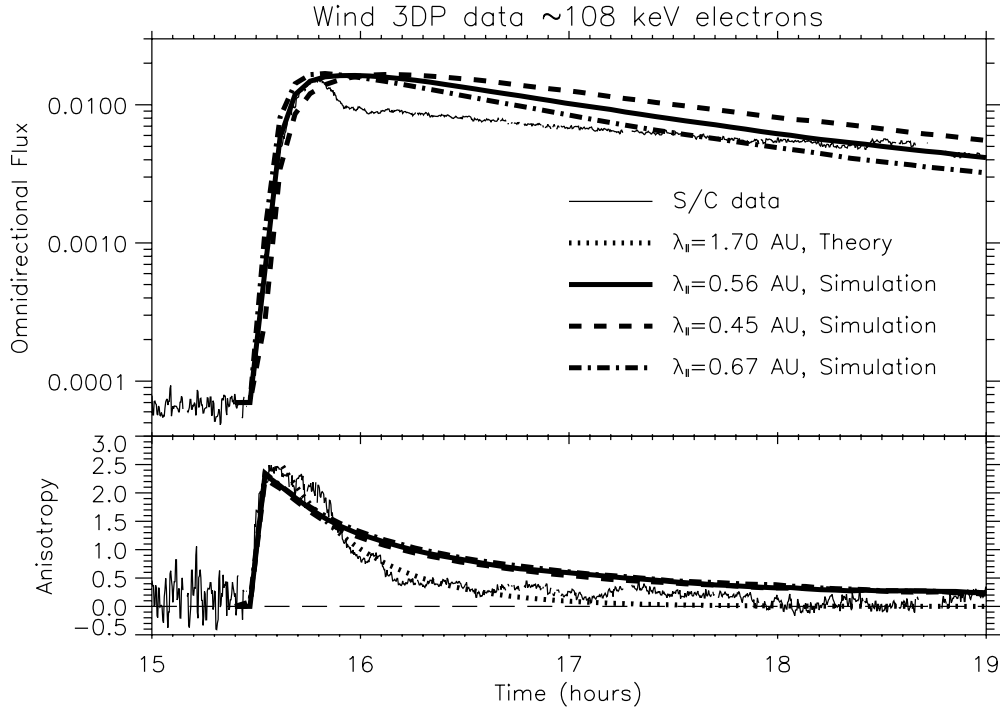


Figure 2. Fits to the flux and anisotropy profiles of *Wind* 3DP ~ 108 keV electron data of the 2000 April 4 event. The form of the pitch-angle diffusion coefficient in Equation (9) is applied in the simulations.

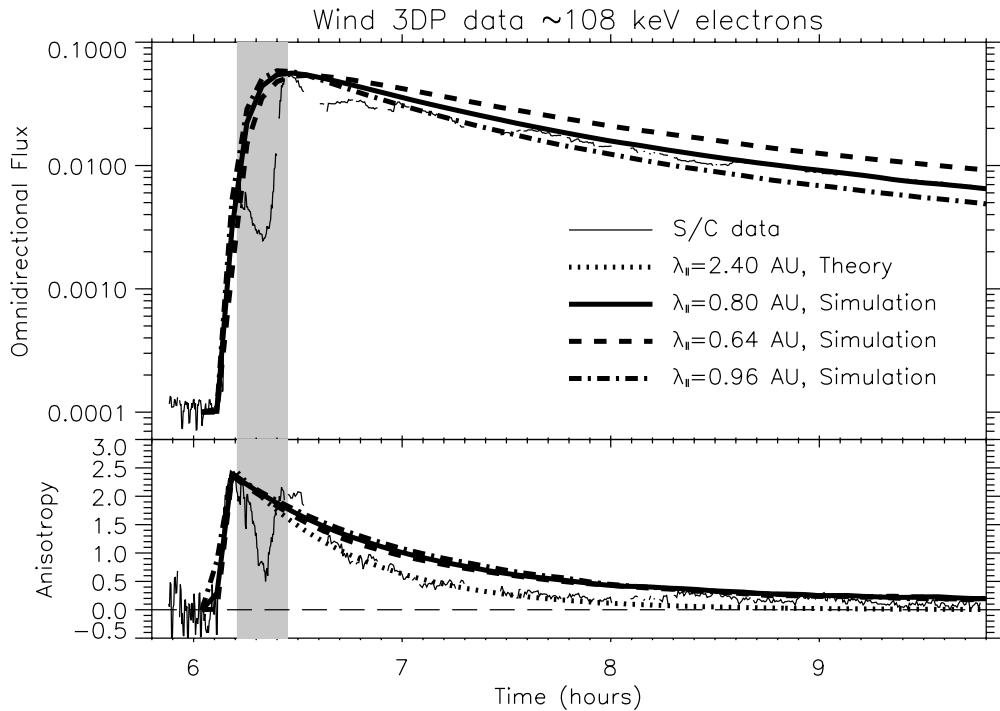


Figure 3. Fits to the flux and anisotropy profiles of *Wind* 3DP ~ 108 keV electron data of the 2002 February 20 event. The form of the pitch-angle diffusion coefficient in Equation (9) is applied in the simulations.

The third impulsive SEP event is the 2002 February 20 solar event observed by the *Wind* 3DP, Case 3. The solar flare associated with this event occurred on $\sim 05:47$ UT at N12W72. We also choose the ~ 108 keV electron channel. Figure 3 shows fits to the flux and anisotropy profiles of this event. In these simulations, we choose $\tau_c = 10$ minutes and $\tau_L = 30$ minutes in Equation (13). The gray vertical shading area in the figure denotes the time period of 6:13–6:27 UT, during which

irregularity was observed. In our simulations for this event, we ignore this time period. As one can see, the thick solid curves (corresponding to $\lambda_{\parallel}^s = 0.80$ AU at 1 AU, i.e., $\lambda_r = 0.36$ AU) fit the observation data best among the three simulations. The parallel mean free paths of the other two simulations are $\lambda_{\parallel}^s = 0.64$ AU and 1 AU (corresponding to $\lambda_r = 0.29$ AU) and $\lambda_{\parallel}^s = 0.96$ AU at 1 AU (corresponding to $\lambda_r = 0.43$ AU); these are the lower and upper limits of the

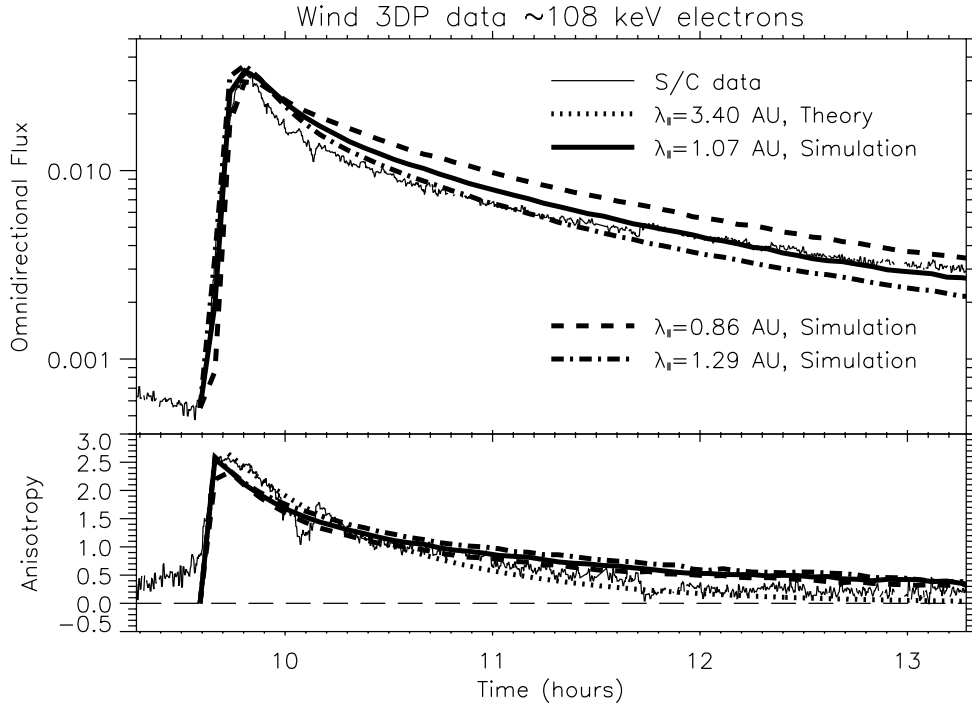


Figure 4. Fits to the flux and anisotropy profiles of *Wind* 3DP ~ 108 keV electron data of the 2000 February 18 event. The form of the pitch-angle diffusion coefficient in Equation (10) is applied in the simulations.

fitted parallel mean free paths. The dotted line in the bottom panel indicates the theoretical result of SEPs' anisotropy. By fitting this analytical result to observations, we obtain that $\mu_0 = 0.81$ and $\lambda_{\parallel}^a = 2.40$ AU in Equation (8). The ratio of the parallel mean free paths of the simulation methods to the analytical method can be obtained for Case 3 as $k_3 = \lambda_{\parallel}^s / \lambda_{\parallel}^a = (0.80 \pm 0.16) / 2.40 = 0.33 \pm 0.07$.

A different form of the pitch-angle diffusion coefficient causes different parallel mean free paths of SEPs by fitting simulations to observations (Qin et al. 2005). Therefore, we also simulate the three impulsive SEP events with other forms of the pitch-angle diffusion coefficient. The next form we use is the pitch-angle diffusion coefficient in Equation (10).

Figure 4 shows fits to the flux and anisotropy profiles of ~ 108 keV electrons in the first event, Case 1. In the simulations for the fitting, we choose $\tau_c = 1$ minute and $\tau_L = 95$ minutes in Equation (13). We can see that, in this figure, the thick solid curves ($\lambda_{\parallel}^s = 1.07$ AU at 1 AU, i.e., $\lambda_r = 0.48$ AU) fit the observation data best among the three simulations. The parallel mean free paths of the other two simulations are $\lambda_{\parallel}^s = 0.86$ AU at 1 AU (corresponding to $\lambda_r = 0.38$ AU) and $\lambda_{\parallel}^s = 1.29$ AU (corresponding to $\lambda_r = 0.58$ AU); these are the lower and upper limits of the fitted parallel mean free paths, respectively. The dotted line in the bottom panel indicates the theoretical result of SEPs' anisotropy, which is the same as that in Figure 1, i.e., $\mu_0 = 0.89$ and $\lambda_{\parallel}^a = 3.40$ AU in Equation (8). For the new form of pitch-angle diffusion, we get the new ratio of parallel diffusion coefficients of the simulation to analytical methods, $k'_1 = \lambda_{\parallel}^s / \lambda_{\parallel}^a = (1.07 \pm 0.22) / 3.40 = 0.31 \pm 0.06$.

We also get new fitted parallel mean free paths with the form of the pitch-angle diffusion coefficient (Equation (10)) for Cases 2 and 3 to get $\lambda_{\parallel}^s = 0.54 \pm 0.11$ AU and 0.77 ± 0.16 AU, respectively (details not shown), and the new ratios $k'_2 = (0.54 \pm 0.11) / 1.70 = 0.32 \pm 0.06$ and $k'_3 = (0.77 \pm 0.16) / 2.40 = 0.32 \pm 0.07$.

Table 1
Comparison of the Parallel Mean Free Path from the Analytical Method and that at 1 AU from the Simulation Methods, with Different Pitch-angle Diffusion Coefficient Models Described by Equations (9), (10), and (6) in the Text

Event	λ_{\parallel}^a (AU) Analytical Method	λ_{\parallel}^s (AU) at 1 AU Simulation Method with $D_{\mu\mu}$ Models		
		Equation (9)	Equation (10)	Equation (6)
1	3.40	1.12 ± 0.22	1.07 ± 0.22	1.01 ± 0.20
2	1.70	0.56 ± 0.11	0.54 ± 0.11	0.50 ± 0.10
3	2.40	0.80 ± 0.16	0.77 ± 0.16	0.72 ± 0.15

Similarly, we also get the new fitted parallel mean free paths with another form of the pitch-angle diffusion coefficient (Equation (6)) for Cases 1, 2, and 3 to get $\lambda_{\parallel}^s = 1.01 \pm 0.20$ AU, 0.50 ± 0.10 AU, and 0.72 ± 0.15 AU, respectively, at 1 AU. So, the new ratio of the simulation to analytical methods for Cases 1, 2, and 3 is $k''_1 = (1.01 \pm 0.20) / 3.40 = 0.30 \pm 0.06$, $k''_2 = (0.50 \pm 0.10) / 1.70 = 0.29 \pm 0.06$, and $k''_3 = (0.72 \pm 0.15) / 2.40 = 0.30 \pm 0.06$, respectively, at 1 AU.

Finally, we show the above results in two tables. Table 1 shows a comparison of the parallel mean free path from the analytical method and the parallel mean free paths at 1 AU from three simulation models with different pitch-angle diffusion coefficients presented in Equations (9), (10), and (6). Table 2 shows the ratio of the parallel mean free paths of the simulation methods to the analytical method. Different ratios are compared with different pitch-angle diffusion coefficient models in the simulation methods. From the two tables, we can see that with different models of the pitch-angle diffusion coefficient, one can obtain different parallel mean free paths from the simulation methods. However, for the SEP events and pitch-angle diffusion models selected for this work, the difference among the results from different pitch-angle models is not

Table 2
Ratio of Parallel Mean Free Paths from Results from the Simulation
Methods to Those from the Analytical Method

Event	$\lambda_{\parallel}^s / \lambda_{\parallel}^a$		
	Simulation Method with $D_{\mu\mu}$ Models		
	Equation (9)	Equation (10)	Equation (6)
1	0.32 ± 0.06	0.31 ± 0.06	0.30 ± 0.06
2	0.33 ± 0.06	0.32 ± 0.06	0.29 ± 0.06
3	0.33 ± 0.07	0.32 ± 0.06	0.30 ± 0.06

Note. Different ratios are compared with different pitch-angle diffusion coefficient models in the simulation methods.

significant. In addition, the results from the analytical method and the simulation methods are significantly different, but the ratio of the mean free paths of the analytical method to the simulation method is about a constant 3.

4. SUMMARY AND CONCLUSION

SEPs' mean free path, determined by physical properties of SEPs as well as those of solar wind, is a very important physical parameter in space weather. To accurately obtain the mean free path of SEPs for a solar event, a so-called simulation method, i.e., fitting time profiles of both flux and anisotropy from spacecraft observations to numerical simulations of SEPs' transport processes, has to be used. However, such fittings and simulations need a large amount of calculation resources; therefore, the simulation method is time-consuming even with modern supercomputers. On the other hand, in space weather practice it is usually necessary to get a quick, approximate estimate of the mean free path. It is necessary to find an alternative way to quickly estimate the mean free path of SEPs.

In this paper, we use a so-called analytical method to quickly estimate SEPs' mean free path by fitting the anisotropy time profiles from the analytical formula of Shalchi et al. (2009) to spacecraft observations. In addition, we compare the mean free path obtained with the traditional simulation method to that obtained with the analytical method to show that the results from the two methods are significantly different, i.e., the ratio of the mean free paths from the analytical method to the simulation method is about 3:1. However, the ratio we obtain is approximately a constant. Moreover, when Shalchi et al. (2009) derived the analytical formula of SEPs' anisotropy time profile (Equation (8)), they used some approximations. Therefore, it is possible to make some modifications to Equation (8) so that it becomes

$$A(t) \approx 3\mu_0 e^{-vt/3\lambda_{\parallel}}. \quad (14)$$

This way, for impulsive events, the new analytical formula can quickly give us a good approximation of SEPs' mean free path that agrees with the mean free paths obtained via the traditional simulation methods.

In addition, the results in this work show that the mean free path obtained with the simulation method depends on the pitch-angle diffusion model used (Qin et al. 2005). However, the pitch-angle diffusion models we use in the simulation method possess strong pitch-angle scattering at $\mu = 0$ to consider not-too-weak magnetic turbulence in solar wind. The mean free paths we obtained with the simulation method do not vary significantly

compared to the fitting uncertainty. Therefore, the analytical method to determine SEPs' mean free path is a useful tool in practice, especially in space weather forecasting. In the future, we will use the new analytical model for more SEP events to determine particles' mean free paths and try to use it to quickly estimate mean free paths in other space weather research.

We were supported in part by the National High-tech R&D Program of China (863 Program) under grant 2010AA122200 and the National Natural Science Foundation of China under grants NNSFC 41074125 and NNSFC 40921063. We benefited from the *Wind* 3DP data provided by the Space Physics Research Group (SPRG), Space Sciences Laboratory (SSL), University of California at Berkeley (<http://sprg.ssl.berkeley.edu/wind3dp/>).

REFERENCES

- Beeck, J., & Wibberenz, G. 1986, *ApJ*, 311, 437
- Bieber, J. W., Matthaeus, W. H., Smith, C. W., Wanner, W., Kallenrode, M.-B., & Wibberenz, G. 1994, *ApJ*, 420, 294
- Dröge, W., & Kartavykh, Y. Y. 2009, *ApJ*, 693, 69
- Dwyer, J. R., et al. 1997, *ApJ*, 490, L115
- Earl, J. A. 1974, *ApJ*, 193, 231
- Freidlin, M. 1985, *Functional Integration and Partial Differential Equations* (Princeton, NJ: Princeton Univ. Press)
- Gardiner, C. 1983, *Handbook of Stochastic Methods for Physics, Chemistry, and the Natural Sciences* (New York: Springer)
- Hasselmann, K., & Wibberenz, G. 1968, *Z. Geophys.*, 34, 353
- Hasselmann, K., & Wibberenz, G. 1970, *ApJ*, 162, 1049
- He, H., Qin, G., & Zhang, M. 2011, *ApJ*, submitted
- Isenberg, P. A. 1997, *J. Geophys. Res.*, 102, 4719
- Jokipii, J. R. 1966, *ApJ*, 146, 480
- Kocharov, L., Vainio, R., Kovaltsov, G. A., & Torsti, J. 1998, *Sol. Phys.*, 182, 195
- Kóta, J. 1997, Proc. 25th ICRC (Durban), Vol. 1, 1, 213
- Lin, R. P., et al. 1995, *Space Sci. Rev.*, 71, 125
- Matthaeus, W. H., Qin, G., Bieber, J. W., & Zank, G. P. 2003, *ApJ*, 590, L53
- Ng, C. K., & Reames, D. V. 1994, *ApJ*, 424, 1032
- Ng, C. K., & Wong, K. Y. 1979, Proc. 16th ICRC, Vol. 5, 252
- Parker, E. N. 1963, *Interplanetary Dynamic Processes* (New York: Interscience)
- Parker, E. N. 1965, *Planet. Space Sci.*, 13, 9
- Qin, G. 2002, PhD thesis, Univ. Delaware
- Qin, G. 2007, *ApJ*, 656, 217
- Qin, G., Matthaeus, W. H., & Bieber, J. W. 2002, *ApJ*, 578, L117
- Qin, G., & Shalchi, A. 2009, *ApJ*, 707, 61
- Qin, G., Zhang, M., & Dwyer, J. R. 2006, *J. Geophys. Res.*, 111, A08101
- Qin, G., Zhang, M., Dwyer, J. R., Rassoul, H. K., & Mason, G. M. 2005, *ApJ*, 627, 562
- Qin, G., Zhang, M., & Rassoul, H. K. 2009, *ApJ*, 114, A09104
- Reid, G. C. 1964, *J. Geophys. Res.*, 69, 2659
- Roelof, E. C. 1969, in *Lectures in High Energy Astrophysics, Propagation of Solar Cosmic Rays in the Interplanetary Magnetic Field*, ed. H. Ogelman & J. R. Wayland (SP-199; Washington, DC: NASA), 111
- Ruffolo, D. 1991, *ApJ*, 382, 688
- Schlickeiser, R. 2002, *Cosmic Ray Astrophysics (Astronomy and Astrophysics Library)*; Berlin: Springer
- Schlüter, W. 1985, PhD thesis, Univ. Kiel
- Shalchi, A. 2005a, *Phys. Plasmas*, 12, 052324
- Shalchi, A. 2005b, *MNRAS*, 363, 107
- Shalchi, A. 2008, *Plasma Phys. Control. Fusion*, 50, 055001
- Shalchi, A. 2009, *Nonlinear Cosmic Ray Diffusion Theories (Astrophysics and Space Science Library, Vol. 362)*; Berlin: Springer
- Shalchi, A., Bieber, J. W., Matthaeus, W. H., & Qin, G. 2004, *ApJ*, 616, 617
- Shalchi, A., Škoda, T., Tautz, R. C., & Schlickeiser, R. 2009, *A&A*, 507, 589
- Skilling, J. 1971, *ApJ*, 170, 265
- Zhang, M. 1999, *ApJ*, 513, 409
- Zhang, M., Jokipii, J. R., & McKibben, R. B. 2003, *ApJ*, 595, 493
- Zhang, M., Qin, G., & Rassoul, H. 2009, *ApJ*, 692, 109